Using low-cost drones to monitor heterogeneous submerged seaweed habitats: a case study in the Azores

Kellaris, Alexandros[1,2], Gil, Artur[3,4*], Faria, João[3,4], Amaral, Ruben[5], Moreu-Badia, Ignacio[3,4], Neto, Ana[3,4] & Yesson, Chris[2*]

[1] Imperial College London, Department of Life Sciences

[2]Institute of Zoology, Zoological Society of London

[3]Universidade dos Açores, Faculdade de Ciências e Tecnologia, Departamento de Biologia

[4]Ce3C - Centre for Ecology, Evolution and Environmental Changes & Azorean Biodiversity Group

[5]DRRF - Direção Regional dos Recursos Florestais, Secretaria Regional da Agricultura e Florestas, Governo Regional dos Açores

*Chris Yesson and Artur Gil are considered joint senior authors

ABSTRACT

1. Remote sensing is a powerful monitoring tool for seaweeds, providing large-scale insights into their ecosystem benefits and invasive impacts. Satellites and manned aircraft have been widely used for this purpose, but their spatial resolution is generally insufficient to map heterogeneous seaweed habitats.
2. In this study, the potential of low-cost and high-resolution drone imagery to map heterogeneous seaweed habitats was assessed on Azorean coasts, where an invasive and commercial species, *Asparagopsis armata,* is present. A Phantom Pro 3 drone equipped with a visible light sensor was used to create photomosaics in three sites on São Miguel island, and ground-truth data for various seaweed groups were collected with exploratory kayak sampling. The support-vector machine, random forest and artificial neural network algorithms were used to construct predictive models of seaweed coverage.
3. Wind, clouds and sun glint were the most significant factors affecting drone surveys and images. Exploratory sampling helped locate relatively homogeneous seaweed patches, however, the data were limited and spatially autocorrelated contributing to over-optimistic model evaluation metrics. Moreover, the models struggled to distinguish seaweeds deeper than three to four metres.
4. In conclusion, using drones to monitor heterogeneous seaweed habitats is challenging, especially in oceanic islands where waters are deep and weather is unpredictable. However, this study highlights the potential use of photo-interpretation to collect modelling data from drone imagery, instead of time-consuming exploratory ground-truth sampling. Future studies could assess drones to map seaweeds in less challenging conditions and use photo-interpretation to improve collection of modelling data.

Key words: coastal; archipelago; remote sensing; monitoring; algae; alien species; aquaculture

1 | INTRODUCTION

Seaweeds are important constituents of coastal habitats, and are often considered to be ecosystem engineers (Jones, Lawton, & Shachak, 1994). Seaweed habitats support high levels of biodiversity (Christie, Norderhaug, & Fredriksen, 2009; Steneck et al., 2002), by providing food (Dayton, 1985; Ince, Hyndes, Lavery, & Vanderklift, 2007), shelter and nursery grounds (Borg, Pihl, & Wennhage, 1997; Duffy & Hay, 1991) to a variety of fish and invertebrates including many commercially exploited

species (Smale, Burrows, Moore, O'Connor, & Hawkins, 2013). Seaweed habitats are also highly productive and support high secondary productivity (Balmford et al., 1973).

Seaweeds provide various ecosystem services to humans, worth billions annually (Beaumont, Austen, Mangi, & Townsend, 2008; Zemke-White & Ohno, 1999). Seaweeds are highly nutritious to humans (Macartain, Gill, Brooks, Campbell, & Rowland, 2007) and produce bioactive compounds used in food, medical and cosmetic products (Holdt & Kraan, 2011; Smit, 2004).

Seaweeds are threatened by various factors. Climate change is expected to affect species distributions, due to the high thermal sensitivity of seaweed survival, growth and reproduction (Harley et al., 2012). Distribution shifts and local extinctions have been observed in some cases (Brodie, Andersen, Kawachi, & Millar, 2009; Simkanin et al., 2005). A meta-analysis in the British Isles showed that seaweed distribution has increased with sea surface temperature in some cases (Yesson, Bush, Davies, Maggs, & Brodie, 2015), although this relationship was not clear. Ocean acidification (Connell & Russell, 2010; Koch, Bowes, Ross, & Zhang, 2013) and increased storminess (Lozano, Devoy, May, & Andersen, 2004) are also expected to negatively affect seaweeds.

Invasive seaweed species also require attention due to their ecological and economic impacts. A meta-analysis (Williams & Smith, 2007) showed that approximately 277 seaweed species have become invasive, introduced mainly through shipping and aquaculture (Schaffelke, Smith, & Hewitt, 2006). Most experimental and observational studies have shown that invasive seaweeds tend to have negative ecological impacts (Schaffelke & Hewitt, 2007; Williams & Smith, 2007), mainly based on their effects on native seaweeds, but these impacts are case-dependent. In general, assessing the ecological impacts of invasive seaweeds is difficult as most research only starts after their introduction (Schaffelke, Smith, & Hewitt, 2006).

The management of beneficial or invasive seaweeds requires monitoring tools to map the spatio-temporal distribution of target species. Traditional approaches such as diving provide high accuracy and resolution, however, they are time-consuming and limited to small areas (Werdell & Roesler, 2003). On the other hand, remote sensing can provide large-scale information of submerged coastal areas in a rapid and cost-effective way (Mumby, Green, Edwards, & Clark, 1999).

Satellites are remote sensing tools frequently used to map seaweeds. Various studies have efficiently used multispectral satellite data to map submerged seaweeds (Andréfouët, Zubia, & Payri, 2004; Casal, Kutser, Domínguez-Gómez, Sánchez-Carnero, & Freire, 2011; Casal, Sánchez-Carnero, Sánchez-Rodríguez, & Freire, 2011; Hoang, O'Leary, & Fotedar, 2016), achieving classification accuracies near the recommended 85% (Congalton & Green, 2009). In general, most studies accomplish broad taxonomic classifications, mainly focusing on brown, red and green seaweed groups. Bio-optical modelling indicates that effective discrimination of submerged red and brown

groups (Kutser, Vahtmäe, & Martin, 2006), and potentially genera or species within these groups, requires fine spectral resolution provided by hyperspectral imagery. The fine spectral resolution presented by multi- and hyper-spectral imagery allows for attenuation correction, which is an important consideration for remote sensing of submerged habitats (Zoffoli et al., 2014). However, a few studies have highlighted the difficulty of using hyperspectral imagery to classify heterogeneous submerged coastal habitats (Casal, Kutser, et al., 2011; Vahtmae & Kutser, 2007). Hyperspectral imagery tends to have low spatial resolution (Govender, Chetty, & Bulcock, 2007), leading to difficulties in mapping highly heterogeneous habitats, submerged or otherwise, due to mixing of spectral information within single pixels. Thus, despite the efficient use of satellites to map submerged seaweeds, higher spatial resolution is required for mapping heterogeneous habitats (Bennion et al., 2018). From a cost perspective, there are coarser resolution (tens of meters) publicly accessible global datasets such as Landsat and Sentinel, but finer scale resolution (1-5m) often requires novel acquisition which incurs substantial costs.

Airborne remote sensing involves collection of aerial imagery from a sensor mounted on an aircraft. The high spatial and spectral resolution of airborne sensors can provide high classification accuracy of submerged aquatic vegetation (Silva, Costa, Melack, & Novo, 2008) and tackle the issue of spatial heterogeneity. Many studies have efficiently used hyperspectral aerial imagery to distinguish red, green and brown groups for floating (Dierssen, Chlus, & Russell, 2015), intertidal (Oppelt, Schulze, Bartsch, Doernhoefer, & Eisenhardt, 2012) and submerged environments (Casal, Kutser, Domínguez-Gómez, Sánchez-Carnero, & Freire, 2013;;; Vahtmäe et al., 2012). However, spectral library modelling has indicated that aerial hyperspectral imagery may be incapable of achieving fine taxonomic resolution in submerged environments due to high spectral similarities (Casal et al., 2013), which can be further complicated by mixing of spectral information in heterogeneous submerged coastal areas (Vahtmae & Kutser, 2007). In addition, the high spatial resolution of typical airborne systems compared to satellites may still be insufficient to map submerged seaweeds in heterogeneous habitats.

Drones, or unmanned aerial vehicles (UAVs), are modern technological advancements which have been increasingly used in the field of ecology (Ventura, Bruno, Jona Lasinio, Belluscio, & Ardizzone, 2016). Drones are airborne systems which can rapidly provide very high spatial resolution images (centimeter scale) of wide areas, providing cost-effective solutions for environmental monitoring (Koh & Wich, 2012). The present UAVs are payload restricted, limiting the sensors available, and most commercial UAVs are fitted with optical cameras. Detailed spectral resolution can be important for distinguishing groups with similar RGB (red, green, blue) optical profiles, and restricting spectral resolution limits the potential for attenuation correction which is improved by hyperspectral data

availability (Zoffoli et al., 2014), although sensor development is proceeding rapidly and a variety of multi-spectral camera systems are available for UAV systems. Compared to satellites and typical airborne systems, drones can provide higher spatial and temporal resolution due to their practicality (but lower spectral resolution), access to remote areas and insensitivity to cloud cover (Paneque-Gálvez, McCall, Napoletano, Wich, & Koh, 2014). In fact, a study comparing remote sensing platforms to map Mediterranean seagrass habitats showed that drone imagery provides the highest spatial accuracy (Ventura, Bonifazi, Gravina, & Ardizzone, 2017), although there is a trade-off between spatial coverage and resolution that must be considered when evaluating methods (Bennion et al. 2018). The high spatial resolution provided by drones could be suitable for mapping heterogeneous seaweed habitats, potentially to fine taxonomic detail due to less spectral mixing.

The red seaweed *Asparagopsis armata*, also known as harpoon weed, is believed to be native to Australia, Tasmania and New Zealand (Horridge, 1951). Its gametophytes have been shown to support rich crustacean assemblages (Pacios, Guerra-García, Baeza-Rojano, & Cabezas, 2011) and produce toxic compounds which deter predators (Paul, De Nys, & Steinberg, 2006).

Currently, *A. armata* is mainly distributed in Oceania, the Mediterranean Sea and European Atlantic coasts, while it is also reported in a few areas in the Americas, Africa and Asia based on the AlgaeBase database (http://www.algaebase.org). *A. armata* has become invasive in the Mediterranean Sea and Eastern Atlantic Ocean, introduced in the 1920s presumably from Australia (Mineur, Davies, Maggs, Verlaque, & Johnson, 2010). In the Mediterranean, it is considered a highly important marine invasive which tends to dominate seaweed canopies (Streftaris & Zenetos, 2006). Moreover, in the Strait of Gibraltar, it has been shown to support less peracarid species than the native *Ellisolandia elongata* (Guerra-García, Ros, Izquierdo, & Soler-Hurtado, 2012).

A. armata is known to produce halogenic and methanolic compounds (McConnell & Fenical, 1977) with antimicrobial (Pesando & Caram, 1984; Salvador, Gómez Garreta, Lavelli, & Ribera, 2007) and anti-cancer properties (Alves, Pinteus, Horta, & Pedrosa, 2016). In fact, it is harvested in seaweed farms in Ireland (Kraan & Barrington, 2005) and Portugal, where it is considered an invasive. Invasive species can be difficult and expensive to manage (Anderson, 2007), so finding commercial incentives to control populations by harvesting can be a valuable approach to management (Pasko & Goldberg, 2014)

A. armata was introduced to the Azores in the early 20th century, where its close relative *A. taxiformis* is also present. Currently, there are ongoing efforts to understand its ecological impacts and potential for commercial exploitation (http://aspazor2016.wixsite.com/aspazor). Rapid monitoring of the distribution and coverage of the species is essential to address these issues.

The aim of this study was to evaluate drones as monitoring tools for seaweeds, applied to the invasive *Asparagopsis armata* in the Azores. The working hypothesis was that low-cost drone imagery can be efficiently used to monitor seaweeds in heterogeneous habitats and potentially distinguish species, owing to its high spatial resolution.

2 | METHODS

2.1 l Study area

The Azores archipelago consists of nine volcanic islands located approximately 1630 km west of Portugal, and situated on top of the Mid-Atlantic Ridge (Figure 1). The islands are mainly formed by basalt rock and surrounded by deep waters within short distances from the coasts. Due to recent volcanic formation, the coastlines tend to have high slopes and irregular shapes, exhibiting semi-diurnal tides with low tidal ranges. The climate is mild yet highly unpredictable due to the influence of the surrounding Atlantic Ocean.

São Miguel is the largest and most densely populated island of the Azores. It is surrounded by rocky shores which are mainly covered by bedrock, cobbles or boulders. The Caloura and Lagoa coasts are located towards the south and have boulder substrates, the latter exhibiting a higher slope (Wallenstein & Neto, 2006). The coast of Mosteiros is located to the north-west, and is covered by bedrock and has a similar slope to Caloura. Wallenstein and Neto (2006) analysed the intertidal biotopes of São Miguel and identified over 70 species of brown, green and red seaweed, mainly growing in turf communities. *A. armata* was found to grow on all substrate types from the lower litteral zone to the subtidal.

The Caloura, Mosteiros and Lagoa coasts were selected for this study due to the high density of *Asparagopsis* species and ease of accessibility. During the period of study, *A. taxiformis* was found to be present in Caloura and Lagoa and *A. armata* in Mosteiros.

2.2 l Drone surveys

The drone surveys were carried out with a low-cost DJI Phantom 3 Professional quadcopter drone (DJI, Shenzhen). The drone's visible light Sony EXMOR camera specifications are provided in the supplementary information. The Phantom 3 was flown once per site around low tide to maximize seaweed exposure to light and under optimal weather conditions, including relatively low cloud cover and wave speed. The DroneDeploy software (DroneDeploy, Florida) was used to design flight plans,

flying at 114 m to achieve an approximate 4.93 cm/pixel resolution in acquired imagery. Such high resolution increased the potential of capturing the smallest of seaweed patches within pixels. The image overlaps were set to 85% frontlap and 80% sidelap. Ground control points (GCPs) were used by taking GPS readings with a handheld GPS/GLONASS receiver (Trimble GeoXT 3.5G, Geoxplorer 6000 series, submetre accuracy) at locations readily identifiable in the aerial images, such as prominent or distinctive rocks on the coastline.

Pix4Dmapper (Pix4D SA, Switzerland) was used to construct photomosaics through stitching the images obtained in each flight and implementing GCPs for accurate georeferencing. The GCPs were initially processed with GPS pathfinder office version 5.6 (Trimble, California) to improve their accuracy up to approximately ±0.5 m. The WGS84/UTM26 (EPSG:32626) coordinate system was used to georeference the images.

A manual mask was applied to each image with QGIS (https://www.qgis.org), to remove pixels corresponding to land. No value adjustment was made to account for brightness variation between the images.

To reduce noise such as shadows, sun glint and foam, the images were converted to greyscale with the average method to find thresholds for pixel removal (Movia, Beinat, & Crosilla, 2016). The thresholds were conservatively set to 35 and 200 based on the greyscale value distribution of noise and non-noise pixels, to prevent removal of the latter. Values below 35 belonged exclusively to shadows, while values above 200 to sun glint and foam.

2.3 l Ground-truth surveys

Kayak surveys were undertaken to collect ground-truth data of each site. The targets involved healthy *Asparagopsis armata*, healthy and decaying *Asparagopsis taxiformis*, brown seaweeds, as well as white substrate, typically a mix of white rock and whitish *Corallina* species. In this case, large homogeneous patches were defined as patches with at least 3 m radius and at least 50% coverage of a particular target. The drone and kayak surveys were organized with a maximum of one day difference to reliably correspond the ground-truth data with the drone images, considering the gradual changes in the abundance of the seaweed targets.

Two transect surveys with exploratory sampling were designed at each site, covering the areas present in the drone images. This targeted sampling design helped collect data representative of each target on these heterogeneous coasts, by sampling areas with high density of a particular target. The surveys involved designing transects above and below the 5 m depth. A snorkeller located large homogeneous targets with a minimum interval of 10 m, taking videos of the patch with an action

camera (GoPro Hero 4, Silver) and estimating depth with a dive computer (Mares Puck Dive Computer). The GPS coordinates for each sample were estimated from a kayak above, with a handheld GPS/GLONASS receiver (Garmin Dakota 20, accuracy ±3 m). The 10 m interval minimized overlap between sampling points, considering the 3m spatial uncertainty of the GPS device.

The videos were qualitatively assessed to determine the approximate proportion of the most frequent target in each ground-truth sample. The samples were included in the analysis only if this proportion exceeded approximately 50%.

2.4 l Image analysis

Supervised classification algorithms were used to construct predictive models of seaweed coverage, through modelling of RGB spectral profiles. The classes were determined both by ground-truthing and photo-interpretation (visual inspection of the images), in some cases including different groups due to spectral similarities (Table 1). The one-vs-one support vector machine (SVM), random forest (RF) and feed-forward artificial neural network (ANN) supervised algorithms were used to classify the drone images, which have been used successfully in other classification studies (Breiman, 2001; Cortes & Vapnik, 1995; Hsu & Lin, 2002; Schmidhuber, 2015).

To improve geospatial accuracy of the ground-truth samples, their location was manually adjusted through detection of visual patterns between the images and underwater videos, such as shapes of rocks or seaweed patches. The pixel values were rescaled to range between 0 and 1 dividing by 255. Each ground-truth point was represented as a circle with 3 m radius around the central location (as shown in Figure 3). All pixels from the aerial imagery that overlapped with this circle were selected as representative of the observed target, including approximately 12320 to 13150 pixels depending on the image. The frequency of each RGB triplet value was examined within this area, and the top 5% of triplet values, corresponding to 5% of the area, were selected as representative of the target. Using the most frequent values minimized the contribution of the less frequent targets and was more reliable than using all values. This method of representative pixel selection was adapted from the methodology used by Brodie, Ash, Tittley, and Yesson (2018).

To train the SVM and ANN algorithms, a five-fold cross validation was undertaken (Hastie, Tibshirani, & Friedman, 2016). Random forest inherently splits the data into bootstrap subsets and uses each subset to construct a decision tree, which is validated on the remaining data (Ho, 1998). The algorithms were evaluated through the mean kappa coefficients of the contingency matrices (Stehman, 1997).

Five-fold cross validation also helped adjust the parameters of SVM (Chang & Lin, 2013) and ANN (Hansen & Salamon, 1990; Krogh & Hertz, 1992) through repeating the process for various parameter combinations and choosing the parameters corresponding to the highest kappa (Table 2). The RF parameters (Breiman, 2001) were adjusted based on the highest kappa acquired through the .632+ bootstrap method (Efron & Tibshirani, 1997).

The data were analysed with the raster (Hijmans, 2017) and caret (Kuhn, 2018) R packages.

3 | RESULTS

3.1 l Drone surveys

Surveys were conducted in May and June 2018. Weather conditions were problematic, highly variable and difficult to predict. Due to time limitations of the project coupled with limited blooming time of *Asparagopsis*, surveys had to be conducted in sub-optimal conditions (waves and clouds). Two hundred to 300 images were taken at each site covering areas between 1/5 - 1/4 km^2 (Table 3). The original and masked Caloura photomosaics are illustrated in Figure 2. Georeferencing the photomosaics using the GCPs resulted in a spatial uncertainty of at least one metre (Root-mean-square error> 1 m). The proportion of pixels identified as noise was 1.5% for Caloura, 0.5% for Lagoa and 0.4% for Mosteiros. The low noise values at Mosteiros obscures the difficulty removing the sun glint affect on the water surface, these were not sufficiently bright to trigger exclusion through the brightness filter (despite a number of attempts varying the thresholds). There remained a noticeable glint effect on the Mosteiros images, but these were analysed regardless.

3.2 l Ground-truth surveys

Ground truth surveys were conducted on days close to the equivalent drone surveys as possible. The sample sizes per target and depth range are presented in Table 4. *A. taxiformis* was found in Caloura and Lagoa, while *A. armata* was only found in Mosteiros. In general, the seabed was highly heterogeneous, but the target coverage in the ground-truth samples was qualitatively determined to exceed 50 %. Two *A. armata* samples were discarded from further analysis due to very low coverage. Example views of *A. armata* samples from aerial and underwater images are presented in Figure 3.

3.3 | Image analysis

Each habitat class was represented in the model training data with between 4940-8279 pixels, based on ground-truthing surveys and photo interpretation (Table 5). *A. armata* shows a relatively dark profile (low values) compared to other classes (Figure 4), in comparison *A. taxiformis* shows a similar escalation of values (R<G<B), but with less variation within each colour. As expected the sand class shows the brightest RGB profile (highest values), and the class of green seaweed is the only class with green values consistently higher than the other bands. Red values are consistently lower than other bands, reflecting greater attenuation of the red light in the water.

These distinct spectral profiles were predicted well by the models. Model evaluation produced consistently high kappa values for all models (Table 6), with consistently high prediction success for all classes (see example contingency matrix for the ANN model in Table 7).

Prediction of habitat classes over the study sites produced a series of habitat maps, an example of the ANN model predictions for the Lagoa region is presented in Figure 5. Predicted area of the target species varies by modelling method (Figure 6), the RF model suggests 5.7 ha of *A. armata was* present in Mosteiros, while the SVM model predicts only 1.8 ha. *A. armata* was not found during ground truthing at Caloura or Lagoa and the models predict almost no habitat at these sites. Predictions of *A. taxiformis* coverage are more consistent, with coverage for Lagoa (where it is most prevalent) between 2.5 ha and 1.8 ha, and at Caloura 0.13-0.16 ha (Figure 6, Table 8).

4 | DISCUSSION

The overall aim of this study was to evaluate drones as monitoring tools for seaweeds, using a low-cost aircraft. Drones can achieve very high spatial resolution which might tackle the issues of habitat heterogeneity and possibly species differentiation, compared to satellites and typical airborne systems. This monitoring methodology was assessed on a species of high importance in the Azores, *Asparagopsis armata*, where the seaweed habitats are highly heterogeneous and closely related species are also present.

4.1 | Drone surveys

The drone surveys in all study sites were strongly affected by weather conditions. In June, rain or drizzle is expected 11 days of the month and the average wind speed is 16 km/h (Weather2 Ltd, 2018),

while DJI suggests not exceeding 20-28 km/h (DJI forum, 2016). Priority was given to days with low wind to fly the drone, and early timing in the morning to minimize sun glint (Mount, 2005). However, clouds were always present to various extents and despite the resulting variation in brightness conditions between the surveys, no effort was made to account for this factor. Flying the drone at similar times of day may be the simplest way of minimizing brightness variation, although this would be dependent on other factors affecting brightness such as time of year (which influences sun direction/height at a given time of day) and cloud cover.

The selection of weather conditions was aimed at minimizing noise due to sun glint, foam and shadows. Optimal conditions were considered to be cloud-free days (or at least days where cloud was unlikely to directly obscure direct sunlight), low wind (i.e. conditions with minimal waves and thus minimal sea foam and glint from wave peaks – optimal wind speeds will vary by exposure of the site and wind direction, but are likely to be substantially lower than the safe operating parameters of the UAV) and limited to several hours around midday to minimise shadows (clearly this is dependent on the time of year and latitude). However, ideal conditions were seldom forthcoming and these issues (glint/foam/shadows) were sometimes evident in images. Some shadows and foam were observed nearby rocks, but were excluded by the noise removal process (Movia et al., 2016). Sun glint on the water surface was an issue for the Mosteiros survey, ideally this would have been re-surveyed but suitable weather conditions (particularly calm seas) were not forthcoming. The result was an over prediction of the sand class in Mosteiros, where it was not observed on the ground surveys. This stresses the importance of surveying in the best possible conditions.

Seaweed and coral remote sensing studies have shown that mixing of spectral information between different groups in heterogeneous coasts limits image classification accuracy (Andréfouët et al., 2004; Caras, Hedley, & Karnieli, 2017; Vahtmae & Kutser, 2007). Specifically, the neighbouring presence of small and spectrally variable patches results in merging of information within single pixels in low spatial resolution images. Caras et al. (2017) suggest using a spatial resolution near the average size of the desired targets to minimize this effect. In this study, a 4.93 cm/pixel resolution was used as a compromise between the potential of capturing individual patches within pixels and practicality. Increasing the resolution would entail flying the drone at a lower altitude, requiring more flight time and possibly causing issues during photomosaic construction (Koh & Wich, 2012).

Georeferencing of the photomosaics had a spatial uncertainty of at least one metre. Spatial accuracy of the photomosaics was important to reliably overlay the ground-truth points on the images, which was further complicated by spatial uncertainty of the latter. However, the high spatial detail in the images made it possible, in many cases, to determine the exact location of seaweed patches in the images through identifying either substrate features, such as rocks, or the exact patches in the

underwater videos. This has strong implications for the accuracy and strategy of the ground-truthing process for drone surveys, as discussed below.

4.2 l Ground-truth surveys

Accurate assignment of ground-truth locations to the image is fundamental to predictive modelling (Brodie et al., 2018). The exploratory sampling strategy helped accurately position the ground-truth classes in the images by targeting large exemplar patches, but might have increased spatial autocorrelation and resulted in over-optimistic model evaluation metrics (Hammond & Verbyla, 1996; Millard & Richardson, 2015). Indeed, the ground-truth points were sometimes clustered and normally collected in limited depth ranges. For example, brown seaweeds and decaying *A. taxiformis* were mainly sampled on top of large rocks near the surface, and *A. armata* samples were clustered within a small area where the species was located. An important observation of this study, however, is the potential of collecting modelling data through detecting shape patterns between the drone and underwater footage. Thus, instead of searching for large homogeneous seaweed patches, it could be possible to implement random or systematic sampling strategies which are less biased and time-consuming. Photo-interpretation can then be used to collect modelling data, although great caution should be given to its subjective nature.

4.3 l Image analysis

The spectral profiles were quite distinct between most classes. An interesting observation was the substantial similarity between the *A. armata* and black rock profiles. Both classes showed dark spectral profiles in drone imagery and this resulted in Amisclassfications between these groups. *A. armata* patches typically displayed bright pink coloration when viewed in underwater imagery, and this red-dominant spectral profile will be significantly affected by attenuation, resulting in difficulties distinguishing this profile when viewed through the water column. Correcting the spectral profile for water depth could be an effective way of combatting this issue (Cho & Lu, 2010), although this would require estimating water depths from the same set of images, which in turn requires ground truthing of water depths (Visser et al., 2015) and employing hyperspectral imaging may improve this method (Lu & Cho, 2011). Depth invariant methods for water column radiometric correction have been proposed (reviewed in Zoffoli et al., 2014), but these methods are dependant on multi- and hyper-spectral data being available, which means RGB imagery from standard optical cameras are not applicable for these methods (Zoffoli et al., 2014). Additionally, techniques of spectral unmixing (e.g.

406 Ettrich et al., 2018) could be employed to help disentangle habitats with similar spectral profiles, but
407 these are best employed when high spectral resolution data (hyperspectral) is available (Hu et al.,
408 2015).
409 This study presents a pixel based classification of the aerial imagery collected. An alternative approach
410 is object-based image analysis (OBIA – e.g. Blaschke, 2010). Habitat mapping using OBIA has increased
411 with the greater availability of higher spatial resolution data, and can be particularly useful where
412 habitat patches are larger the pixels of the remote sensing data (Blaschke, 2010). OBIA can reduce the
413 'salt and pepper' effect often seen in pixel-based methods of classification and can utilise more
414 features than isolated pixel values by incorporating contextual information for classification (Benz,
415 2004).
416 An important question of this study was whether the high resolution of drone imagery can help
417 distinguish closely related species, partly due to less spectral mixing. The underwater footage showed
418 that *A. taxiformis* displayed a darker coloration than *A. armata*. The spectral profiles between the
419 *Asparagopsis* species were also distinct, but this is difficult to explain solely based on coloration
420 differences between the species. In any case, acquiring the pure profiles of seaweeds in
421 heterogeneous habitats is complicated by the difficulty of determining their exact pixel location. The
422 methodology of representative pixel extraction (Brodie et al., 2018) applied in this study to deal with
423 spatial uncertainty and patch heterogeneity assumes that the extracted pixels are representative of
424 the desired target. Extracting the top 5% of ground-truth circle values was a compromise between
425 sample size and target representativity. In this sense, it is not clear to what extent the profiles were
426 representative of the classes. Thus, this work is limited in its ability to address the potential of drone
427 visible light imagery to distinguish the *Asparagopsis* species, and closely related species in general.
428 The models showed very high evaluation metrics indicating overfitting to the training data.
429 Overfitting might have been partly caused by the presence of relatively few distinct values per class in
430 the 5% dataset. Objectively evaluating the generalizability of a trained model requires testing on a
431 distinct validation dataset (Witten & Frank, 2005). Radosavljevic and Anderson (2014) suggest using a
432 geographically masked cross-validation approach to evaluate training data on validation data collected
433 in different regions. However, in this study each class was typically present only at one site, and the
434 samples were too few to create spatial partitions within each site. Thus, both spatial autocorrelation
435 and limited values might have contributed to model overfitting.
436 An interesting observation was the heterogeneity of classifications in deep waters compared to
437 shallower waters. In fact, deeper than three to four metres, the models typically predicted a single
438 class indicating the difficulty of separating targets in such depths. This was likely amplified by the

shortness of turf-forming seaweeds dominating the Azorean coasts (Wallenstein & Neto, 2006), compared to canopy-forming species.

4.4 l Monitoring and management implications

An important goal of this project was to develop models predicting *A. armata* coverage in drone imagery, to monitor the abundance and distribution of this invasive in the Azores. Unfortunately, we feel that, at present, our approach is not sufficient to produce reliable models for this study. This should not discourage others from attempting other drone-based monitoring as there are some particular issues with the Azores and *Asparagopsis* that inhibited this study. The short-lived gametophyte phase places a particular time-pressure on surveys, which are further confounded by highly unpredictable, oceanic weather. Monitoring targets with year-round visible presence, in friendlier climates would make more obvious targets for similar studies.

There are many advantages to drone-based monitoring, such as the relative low-cost, accessibility and practicality which may facilitate monitoring. The repeated monitoring of sites where invasive species are known or suspected to be a threat could be a valuable tool for invasive management. However, there are cost considerations beyond the price of the UAV hardware, these may include equipment for high spatial precision georeferencing (cm scale), training to safely operate equipment, specialised software (such as Pix4D) and computing resources for mass processing of imagery, as well as the time required for image acquisition and analysis. These associated costs will inevitable come down making studies more practical and reliable with improved technology, incorporating more sensors, and improved methods for processing imagery (Bennion et al. 2018).

5 l CONCLUSIONS

An important conclusion of the study is that using drones to monitor the turfy and highly heterogeneous seaweed habitats of the Azores is challenging, which may extend to similar habitats and other oceanic islands. Firstly, collecting accurate ground-truth data in such habitats is challenging and complicates the development of efficient predictive models. In addition, despite the practicality of drones, the unpredictable weather limits their spatio-temporal flexibility and flights are restricted to early morning or evening to avoid sun glint. It is also worth noting that the shortness of turfy seaweeds amplified by the high slope of oceanic islands limits monitoring to a small distance from the shore.

Despite these limitations, an important implication of this work is the potential use of photo-interpretation to collect accurate modelling data from drone imagery. Pattern detection between aerial and underwater footage can reduce the necessity of explorative ground-truth surveys in such cases, encouraging systematic or random surveys which are less biased and time-consuming.

This study was implemented in challenging geographic and weather conditions, confounded by the short-lived target species. In areas with more stable and predictable weather, and with long-enduring monitoring targets, drones should be efficient tools for monitoring seaweeds. .

ACKNOWLEDGMENTS

This study is a contribution to the research project 'ASPAZOR – Ecosystem impacts and socioeconomic benefits of *Asparagopsis armata* in the Azores' (Ref. ACORES-01-1045-FEDER-00060) funded through FEDER (85%) and Regional funds (15%) via "Programa Operacional Açores 2020". Alexandros Kellaris was supported by Imperial College London with a project budget for his Masters thesis. The participation of co-author Artur Gil in this study was supported by the Post-Doctoral Research Project SFRH/BPD/100017/2014 from FCT, funded by the National Budget of the Ministry of Education and Science of Portugal and by the European Social Fund. The authors thank Anabela Isidoro, Vasco Medeiros, João Luis Pacheco and the overall institutional support from the DRRF - "Direção Regional de Recursos Florestais".

REFERENCES

Alves, C., Pinteus, S., Horta, A., & Pedrosa, R. (2016). High cytotoxicity and anti-proliferative activity of algae extracts on an in vitro model of human hepatocellular carcinoma. *SpringerPlus*, 5. 1339

Anderson, L. W. J. (2007). Control of invasive seaweeds. *Botanica Marina*, 50, 418–437.

Andréfouët, S., Zubia, M., & Payri, C. (2004). Mapping and biomass estimation of the invasive brown algae Turbinaria ornata (Turner) J. Agardh and Sargassum mangarevense (Grunow) Setchell on heterogeneous Tahitian coral reefs using 4-meter resolution IKONOS satellite data. *Coral Reefs*, 23, 26–38.

Balmford, A., Bennun, L., Brink, B., Cooper, D., Côté, I. M., Crane, P., … Walther, B. A. (1973). Seaweeds: Their productivity and strategy for growth. *Science*, 182, 14–16.

Beaumont, N. J., Austen, M. C., Mangi, S. C., & Townsend, M. (2008). Economic valuation for the conservation of marine biodiversity. *Marine Pollution Bulletin*, 56, 386–396.

506 Bennion, M., Fisher, J., Yesson, C., & Brodie, J. (2019). Remote Sensing of Kelp (Laminariales,
507 Ochrophyta): Monitoring Tools and Implications for Wild Harvesting. *Reviews in Fisheries*
508 *Science & Aquaculture*, 27, 127-141.
509 Benz, U.C. (2004). Multi-resolution, object-oriented fuzzy analysis of remote sensing data for GIS-
510 ready information. *ISPRS Journal of Photogrammetry and Remote Sensing*, 58, 239– 258.
511 Blaschke, T. (2010). Object based image analysis for remote sensing. *ISPRS Journal of*
512 *Photogrammetry and Remote Sensing*, 65, 2-16.
513 Borg, A., Pihl, L., & Wennhage, H. (1997). Habitat choice by juvenile cod (Gadus morhua L .) on
514 sandy soit bottoms with different vegetation types. *Helgoländer Meeresuntersuchungen*, 51,
515 197–212.
516 Breiman, L. (2001). Random forests. *Machine Learning*, 45, 5–32.
517 Brodie, J., Andersen, R. A., Kawachi, M., & Millar, A. J. K. (2009). Endangered algal species and how
518 to protect them. *Phycologia*, 48, 423–438.
519 Brodie, J., Ash, L. V., Tittley, I., & Yesson, C. (2018). A comparison of multispectral aerial and satellite
520 imagery for mapping intertidal seaweed communities. *Aquatic Conservation: Marine and*
521 *Freshwater Ecosystems*, 28, 872–881.
522 Caras, T., Hedley, J., & Karnieli, A. (2017). Implications of sensor design for coral reef detection:
523 Upscaling ground hyperspectral imagery in spatial and spectral scales. *International Journal of*
524 *Applied Earth Observation and Geoinformation*, 63, 68–77.
525 Casal, G., Kutser, T., Domínguez-Gómez, J. A., Sánchez-Carnero, N., & Freire, J. (2011). Mapping
526 benthic macroalgal communities in the coastal zone using CHRIS-PROBA mode 2 images.
527 *Estuarine, Coastal and Shelf Science*, 94, 281–290.
528 Casal, G., Kutser, T., Domínguez-Gómez, J. A., Sánchez-Carnero, N., & Freire, J. (2013). Assessment of
529 the hyperspectral sensor CASI-2 for macroalgal discrimination on the Ría de Vigo coast (NW
530 Spain) using field spectroscopy and modelled spectral libraries. *Continental Shelf Research*, 55,
531 129–140.
532 Casal, G., Sánchez-Carnero, N., Sánchez-Rodríguez, E., & Freire, J. (2011). Remote sensing with SPOT-
533 4 for mapping kelp forests in turbid waters on the south European Atlantic shelf. *Estuarine,*
534 *Coastal and Shelf Science*, 91, 371–378.
535 Chang, C., & Lin, C. (2013). LIBSVM : A Library for Support Vector Machines. *ACM Transactions on*
536 *Intelligent Systems and Technology (TIST)*, 2, 1–39.
537 Cho, H.J., & Lu, D.J. (2010) A water-depth correction algorithm for submerged vegetation spectra.
538 *Remote Sensing Letters*, 1, 29-35.
539 Christie, H., Norderhaug, K. M., & Fredriksen, S. (2009). Macrophytes as habitat for fauna. *Marine*

Ecology Progress Series, *396*, 221–233.

Congalton, R., & Green, K. (2009). *Assessing the Accuracy of Remotely Sensed Data* (2nd ed.). Florida: CRC Press.

Connell, S. D., & Russell, B. D. (2010). The direct effects of increasing CO2 and temperature on non-calcifying organisms: increasing the potential for phase shifts in kelp forests. *Proceedings of the Royal Society B: Biological Sciences*, 277, 1409–1415.

Cortes, C., & Vapnik, V. (1995). Support Vector Networks. *Machine Learning*, 20, 273-297.

Dayton, P. K. (1985). Ecology of kelp communities. *Annual Review of Ecology and Systematics*, *16*, 212–245.

Dierssen, H. M., Chlus, A., & Russell, B. (2015). Hyperspectral discrimination of floating mats of seagrass wrack and the macroalgae Sargassum in coastal waters of Greater Florida Bay using airborne remote sensing. *Remote Sensing of Environment*, 167, 247–258.

DJI forum. (2016). https://forum.dji.com/thread-48223-1-1.html/ [14 May 2018]

Duffy, E., & Hay, M. E. (1991). Food and shelter as determinants of food choice by an herbivorous marine amphipod. *Ecology*, 72, 1286–1298.

Efron, B., & Tibshirani, R. (1997). Improvements on cross-validation: The .632+ bootstrap method. *Journal of the American Statistical Association*, 92, 548–560.

Ettritch, G., Bunting, P., Jones, G. & Hardy, A. (2018). Monitoring the coastal zone using earth observation: application of linear spectral unmixing to coastal dune systems in Wales. *Remote Sensing in Ecology and Conservation*, 4, 303-319.

Govender, M., Chetty, K., & Bulcock, H. (2007). A review of hyperspectral remote sensing and its application in vegetation and water resource studies. *Water SA*, 33, 145–151.

Guerra-García, J. M., Ros, M., Izquierdo, D., & Soler-Hurtado, M. M. (2012). The invasive Asparagopsis armata versus the native Corallina elongata: Differences in associated peracarid assemblages. *Journal of Experimental Marine Biology and Ecology*, 416–417, 121–128.

Hammond, T. O., & Verbyla, D. L. (1996). Optimistic bias in classification accuracy assessment. *International Journal of Remote Sensing*, 17, 1261–1266.

Hansen, L. K., & Salamon, P. (1990). Neural Network Ensembles. *IEEE Transactions on Pattern Analysis and Machine Intelligence*, 12, 993–1001.

Harley, C. D. G., Anderson, K. M., Demes, K. W., Jorve, J. P., Kordas, R. L., Coyle, T. A., & Graham, M. H. (2012). Efects Of Climate Change On Global Seaweed Communities. *Journal of Phycology*, 48, 1064–1078.

Hastie, T., Tibshirani, R. J., & Friedman, J. H. (2016). Model Assessment and Selection. In *The Elements of Statistical Learning* (2nd ed.). New York: Springer.

574 Hijmans, R. J. (2017). raster: Geographic Data Analysis and Modeling. R package version 2.6-7.
575 https://CRAN.R-project.org/package=raster.
576 Ho, T. K. (1998). The random subspace method for constructing decision forests. *IEEE Transactions*
577 *on Pattern Analysis and Machine Intelligence*, 20, 832–844.
578 Hoang, T. C., O'Leary, M. J., & Fotedar, R. K. (2016). Remote-Sensed Mapping of *Sargassum* spp.
579 Distribution around Rottnest Island, Western Australia, Using High-Spatial Resolution
580 WorldView-2 Satellite Data. *Journal of Coastal Research*, 322, 1310–1321.
581 Holdt, S. L., & Kraan, S. (2011). Bioactive compounds in seaweed : functional food applications and
582 legislation. *Journal of Applied Phycology*, 23, 543–597.
583 Horridge, G. A. (1951). Occurrence of Asparagopsis armata Harv. on the Scilly Isles. *Nature*, 167,
584 732–733.
585 Hsu, C., & Lin, C. (2002). A comparison of methods for multiclass support vector machines. *Neural*
586 *Networks, IEEE Transactions on Neural Networks*, 13, 415–425.
587 Hu, C.M., Feng, L., Hardy, R.F. & Hochberg, E.J. (2015). Spectral and spatial requirements of remote
588 measurements of pelagic Sargassum macroalgae. *Remote Sensing of Environment*, 167, 229-
589 246.
590 Ince, R., Hyndes, G. A., Lavery, P. S., & Vanderklift, M. A. (2007). Marine macrophytes directly
591 enhance abundances of sandy beach fauna through provision of food and habitat. *Estuarine,*
592 *Coastal and Shelf Science*, 74, 77–86.
593 Jones, C. G., Lawton, J. H., & Shachak, M. (1994). Organisms as ecosystem engineers. *Oikos*, 69, 373–
594 386.
595 Koch, M., Bowes, G., Ross, C., & Zhang, X. H. (2013). Climate change and ocean acidification effects
596 on seagrasses and marine macroalgae. *Global Change Biology*, 19, 103–132.
597 Koh, L. P., & Wich, S. A. (2012). Dawn of drone ecology: low-cost autonomous aerial vehicles for
598 conservation. *Tropical Conservation Science*, 5, 121–132.
599 Kraan, S., & Barrington, K. A. (2005). Commercial farming of Asparagopsis armata
600 (Bonnemaisoniceae, Rhodophyta) in Ireland, maintenance of an introduced species? *Journal of*
601 *Applied Phycology*, 17, 103–110.
602 Krogh, A., & Hertz, J. A. (1992). A Simple Weight Decay Can Improve Generalization. *Advances in*
603 *Neural Information Processing Systems*, 4, 950–957.
604 Kuhn, M. 2018. caret: Classification and Regression Training. R package version 6.0-79.
605 https://CRAN.R-project.org/package=caret.
606 Kutser, T., Vahtmäe, E., & Martin, G. (2006). Assessing suitability of multispectral satellites for
607 mapping benthic macroalgal cover in turbid coastal waters by means of model simulations.

608 *Estuarine, Coastal and Shelf Science*, 67, 521–529.
609 Lozano, I., Devoy, R. J. N., May, W., & Andersen, U. (2004). Storminess and vulnerability along the
610 Atlantic coastlines of Europe: Analysis of storm records and of a greenhouse gases induced
611 climate scenario. *Marine Geology*, 210, 205–225.
612 Lu, D.J., & Cho, H.J. (2011) An improved water-depth correction algorithm for seagrass mapping
613 using hyperspectral data. *Remote Sensing Letters*, 2, 91-97.
614 Macartain, P., Gill, C. I. R., Brooks, M., Campbell, R., & Rowland, I. R. (2007). Nutritional Value of
615 Edible Seaweeds. *Nutrition Reviews*, 65, 535–543.
616 McConnell, O., & Fenical, W. (1977). Halogen chemistry of the red alga Asparagopsis.
617 *Phytochemistry*, 16, 367–374.
618 Millard, K., & Richardson, M. (2015). On the importance of training data sample selection in Random
619 Forest image classification: A case study in peatland ecosystem mapping. *Remote Sensing*, 7,
620 8489–8515.
621 Mineur, F., Davies, A. J., Maggs, C. A., Verlaque, M., & Johnson, M. P. (2010). Fronts, jumps and
622 secondary introductions suggested as different invasion patterns in marine species, with an
623 increase in spread rates over time. *Proceedings of the Royal Society B: Biological Sciences*, 277,
624 2693–2701.
625 Mount, R. (2005). Acquisition of Through-water Aerial Survey Images : Surface Effects and the
626 Prediction of Sun Glitter and Subsurface Illumination. *Photogrammetric Engineering & Remote*
627 *Sensing*, 71, 1407–1415.
628 Movia, A., Beinat, A., & Crosilla, F. (2016). Shadow detection and removal in RGB VHR images for
629 land use unsupervised classification. *ISPRS Journal of Photogrammetry and Remote Sensing*,
630 119, 485–495.
631 Mumby, P. J., Green, E. P., Edwards, A. J., & Clark, C. D. (1999). The cost-effectiveness of remote
632 sensing for tropical coastal resources assessment and management. *Journal of Environmental*
633 *Management*, 55, 157–166.
634 Oppelt, N., Schulze, F., Bartsch, I., Doernhoefer, K., & Eisenhardt, I. (2012). Hyperspectral
635 classification approaches for intertidal macroalgae habitat mapping : a case study in
636 Heligoland. *Optical Engineering*, 51, 111703.
637 Pacios, I., Guerra-García, J. M., Baeza-Rojano, E., & Cabezas, M. P. (2011). The non-native seaweed
638 Asparagopsis armata supports a diverse crustacean assemblage. *Marine Environmental*
639 *Research*, 71, 275–282.
640 Paneque-Gálvez, J., McCall, M. K., Napoletano, B. M., Wich, S. A., & Koh, L. P. (2014). Small drones
641 for community-based forest monitoring: An assessment of their feasibility and potential in

642 tropical areas. *Forests*, 5, 1481–1507.
643 Pasko, S., & Goldberg, J. (2014). Review of harvest incentives to control invasive species.
644 *Management of Biological Invasions*, 5, 263–277.
645 Paul, N. A., De Nys, R., & Steinberg, P. D. (2006). Seaweed-herbivore interactions at a small scale:
646 Direct tests of feeding deterrence by filamentous algae. *Marine Ecology Progress Series*, 323,
647 1–9.
648 Pesando, D., & Caram, B. (1984). Screening of marine algae from the French Mediterranean coast for
649 antibacterial and antifungal activity. *Botanica Marina*, 27, 381–386.
650 Radosavljevic, A., & Anderson, R. P. (2014). Making better Maxent models of species distributions:
651 Complexity, overfitting and evaluation. *Journal of Biogeography*, 41, 629–643.
652 Salvador, N., Gómez Garreta, A., Lavelli, L., & Ribera, M. A. (2007). Antimicrobial activity of Iberian
653 macroalgae. *Scientia Marina*, 71, 101–114.
654 Schaffelke, B., & Hewitt, C. L. (2007). Impacts of introduced seaweeds. *Botanica Marina*, 50, 397–
655 417.
656 Schaffelke, B., Smith, J. E., & Hewitt, C. L. (2006). Introduced macroalgae - A growing concern.
657 *Journal of Applied Phycology*, 18, 529–541.
658 Schmidhuber, J. (2015). Deep Learning in neural networks: An overview. *Neural Networks*, 61, 85–
659 117.
660 Silva, T. S. F., Costa, M. P. F., Melack, J. M., & Novo, E. M. L. M. (2008). Remote sensing of aquatic
661 vegetation: theory and applications. *Environmental Monitoring and Assessment*, 140, 131–145.
662 Simkanin, C., Power, A., Myers, A., McGrath, D., Southward, A., Mieszkowska, N., … O'Riordan, R.
663 (2005). Using historical data to detect temporal changes in the abundances of intertidal species
664 on Irish shores. *Journal of the Marine Biological Association of the United Kingdom*, 85, 1329–
665 1340.
666 Smale, D. A., Burrows, M. T., Moore, P., O'Connor, N., & Hawkins, S. J. (2013). Threats and
667 knowledge gaps for ecosystem services provided by kelp forests: A northeast Atlantic
668 perspective. *Ecology and Evolution*, 3, 4016–4038.
669 Smit, A. J. (2004). Medicinal and pharmaceutical uses of seaweed natural products: A review. *Journal*
670 *of Applied Phycology*, 16, 245-262.
671 Stehman, S. V. (1997). Selecting and interpreting measures of thematic classification accuracy.
672 *Remote Sensing of Environment*, 62, 77–89.
673 Steneck, R. S., Graham, M. H., Bourque, B. J., Corbett, D., Erlandson, J. M., Estes, J. A., & Tegner, M. J.
674 (2002). Kelp forest ecosystems: Biodiversity, stability, resilience and future. *Environmental*
675 *Conservation*, 29, 436–459.

676 Story, M., & Congalton, R. G. (1986). Accuracy assessment: a user's perspective. *Photogrammetric*
677 *Engineering & Remote Sensing*, 52, 397–399.
678 Streftaris, N., & Zenetos, A. (2006). Alien marine species in the Mediterranean - the 100 'worst
679 invasives' and their impact. *Mediterranean Marine Science*, 7, 87–118.
680 Vahtmae, E., & Kutser, T. (2007). Mapping Bottom Type and Water Depth in Shallow Coastal Waters
681 with Satellite Remote Sensing. *Journal of Coastal Research*, 2007, 185–189.
682 Vahtmäe, E., Kutser, T., Kotta, J., Pärnoja, M., Möller, T., & Lennuk, L. (2012). Mapping Baltic Sea
683 Shallow Water Environments with Airborne Remote Sensing. *Oceanology*, 52, 803–809.
684 Ventura, D., Bonifazi, A., Gravina, M. F., & Ardizzone, G. D. (2017). Unmanned Aerial Systems (UASs)
685 for Environmental Monitoring: A Review with Applications in Coastal Habitats. In *Aerial Robots*
686 *- Aerodynamics, Control and Applications*. InTechOpen.
687 Ventura, D., Bruno, M., Jona Lasinio, G., Belluscio, A., & Ardizzone, G. (2016). A low-cost drone based
688 application for identifying and mapping of coastal fish nursery grounds. *Estuarine, Coastal and*
689 *Shelf Science*, 171, 85–98.
690 Visser, F., Buis, K., Verschoren, V., & Meire, P. (2015) Depth Estimation of Submerged Aquatic
691 Vegetation in Clear Water Streams Using Low-Altitude Optical Remote Sensing. *Sensors*, 15,
692 25287-25312.
693 Wallenstein, F. F. M. M., & Neto, A. I. (2006). Intertidal rocky shore biotopes of the Azores: A
694 quantitative approach. *Helgoland Marine Research*, 60, 196–206.
695 Weather2 Ltd. 2018. http://www.myweather2.com/Holiday-Destinations/Azores-Islands/Ponta-
696 Delgada/climate-profile.aspx?month=6/ [10 May 2018]
697 Werdell, P. J., & Roesler, C. S. (2003). Remote assessment of benthic substrate composition in
698 shallow waters using multispectral reflectance. *Limnology and Oceanography*, 48, 557–567.
699 Williams, S. L., & Smith, J. E. (2007). A Global Review of the Distribution, Taxonomy, and Impacts of
700 Introduced Seaweeds. *Annual Review of Ecology, Evolution, and Systematics*, 38, 327–359.
701 Witten, I. H., & Frank, E. (2005). Credibility: Evaluating what's been learned. In *Data Mining: Practical*
702 *Machine Learning Tools and Techniques* (2nd ed., pp. 143–185). San Fransisco: Elsevier.
703 Yesson, C., Bush, L. E., Davies, A. J., Maggs, C. A., & Brodie, J. (2015). Large brown seaweeds of the
704 british isles: Evidence of changes in abundance over four decades. *Estuarine, Coastal and Shelf*
705 *Science*, 155, 167–175.
706 Zemke-White, W. L., & Ohno, M. (1999). World seaweed utilisation: An end-of-century summary.
707 *Journal of Applied Phycology*, 11, 369–376.
708 Zoffoli, M.L., Frouin, R. & Kampel, M. (2014). Water Column Correction for Coral Reef Studies by
709 Remote Sensing. *Sensors*, 14(9), 16881-16931.

TABLES AND FIGURES

TABLE 1

Description and data source of classes used in classification

Class	Description	Source
A. armata	*A. armata* in its reddish state	Ground-truth
A. taxiformis	Reddish *A. taxiformis*	Ground-truth
Brown	Brown seaweeds and decaying *A. taxiformis* in a brownish state	Ground-truth
Deep	Deep samples (>5m) and white substrate (white rock and *Corallina*)	Ground-truth
Green	Green seaweeds and the yellowish *Cystoseira abies-marina*	Photointerpretation
Black rock	Black basalt rock	Photointerpretation
Sand	White sand	Photointerpretation

TABLE 2

Parameter combinations tested with five-fold cross validation for SVM and ANN, and 0.632+ bootstrapping for RF

SVM		RF		ANN	
Gamma	*Cost*	*Trees*	*Features*	*Neurons*	*Weight decay*
$\mathbf{2^{-13}}$ **-** $\mathbf{2^{-12}}$ **-...-** $\mathbf{2^{3}}$	2^{-6} - 2^{-5} -...- 2^{13}	50 - 100 - 200 - 500	1 - 2	1 - 2 - 3 - 4 -5	0 - 0.01 - 0.1 - 0.5

TABLE 3

Flight specifications for the Caloura, Mosteiros and Lagoa study sites

	Caloura	Lagoa	Mosteiros
Target altitude (m)	114	114	114
Target resolution (cm/pixel)	4.93	4.93	4.93
Total area (km^2)	0.247	0.251	0.197
Images	335	314	204

GCPs	4	4	4

TABLE 4

Ground-truth sample size for each target and depth range

Target	Shallow (0-5m)	Deep (>5m)
A. armata	10	-
***A. taxiformis* (healthy)**	9	-
***A. taxiformis* (decaying)**	8	-
Brown seaweeds	6	2
White substrate	8	2

TABLE 5

Classification sample sizes as pixels and circles (ground-truth classes only)

Class	Pixels	Circles
A. armata	4940	8
A. taxiformis	5928	9
Brown	8279	14
Green	6138	-
Sand	6538	-
Black rock	6162	-
Deep	5133	12

TABLE 6

Kappa statistics and optimal parameters obtained through five-fold cross validation for SVM and ANN, and 0.632+ bootstrapping for RF

Kappa (%)	SVM		RF		ANN	
Mean ± SD	0.998 ± 6.42e-4		0.998 ± 4.27e-4		0.983 ± 4.91e-3	
Parameters	Gamma	Cost	Trees	Features	Neurons	Weight decay
Value	8	8192	500	2	5	0.1

TABLE 7

Contingency matrix for ANN tested on the whole training dataset

Actual class	*Predicted class*							*Producer accuracy (%)*
	A. armata	*A. taxiformis*	Brown	Green	Deep	Sand	Black rock	
A. armata	4751	0	0	0	0	0	189	0.96
A. taxiformis	0	5814	114	0	0	0	0	0.98
Brown	0	0	8279	0	0	0	0	1
Green	22	0	0	6110	0	0	6	0.99
Deep	0	0	0	0	5133	0	0	1
Sand	0	0	0	0	0	6538	0	1
Black rock	5	0	243	0	0	0	5914	0.95
User accuracy (%)	0.99	1	0.95	1	1	1	0.96	***Total accuracy*** 0.98 %

741 **TABLE 8**

742 Class proportions per location as predicted by RF, ANN and SVM. Total area refers to non-masked area
743 estimated with the S.1 formula.

RF	***A. armata***	***A. taxiformis***	**Brown**	**Green**	**Deep**	**Sand**	**Black rock**	**Total area (km²)**
Caloura	<0.001	0.097	0.097	0.054	0.434	0.202	0.097	0.160
Lagoa	0.009	0.240	0.073	0.073	0.319	0.103	0.174	0.106
Mosteiros	0.445	0.046	0.012	0.098	0.023	0.049	0.319	0.126
ANN								
Caloura	0.002	0.099	0.236	0.073	0.434	0.013	0.063	0.160
Lagoa	0.049	0.239	0.115	0.166	0.319	0.066	0.045	0.106
Mosteiros	0.382	0.040	0.031	0.389	0.023	0.019	0.118	0.126
SVM								
Caloura	<0.001	0.087	0.065	0.348	0.35	<0.001	0.132	0.160
Lagoa	0.002	0.170	0.038	0.280	0.305	0.047	0.148	0.106
Mosteiros	0.142	0.010	0.002	0.620	0.011	0.007	0.200	0.126

744

745

FIGURE 1 Location of the Azores, São Miguel and study sites: Mosteiros, Lagoa and Caloura (Europe coastline data, European Environment Agency, https://www.eea.europa.eu)

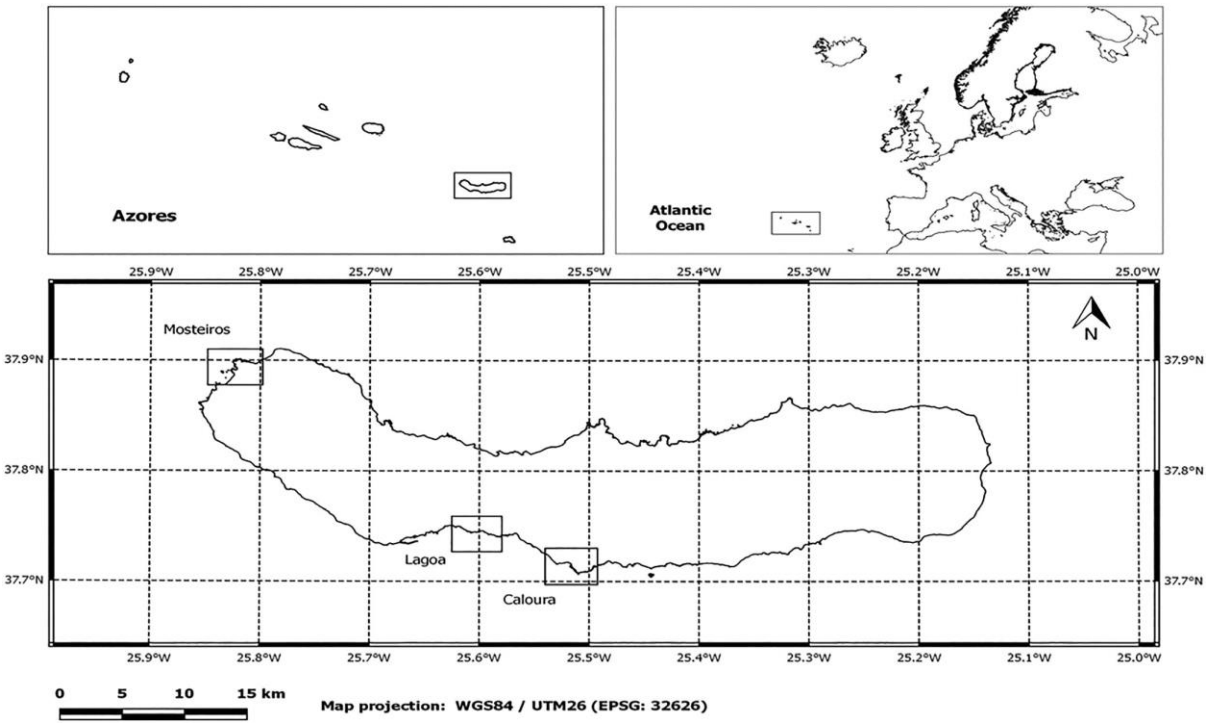

750 **FIGURE 2.** Original (left) and masked (right) versions of the Caloura photomosaic

751

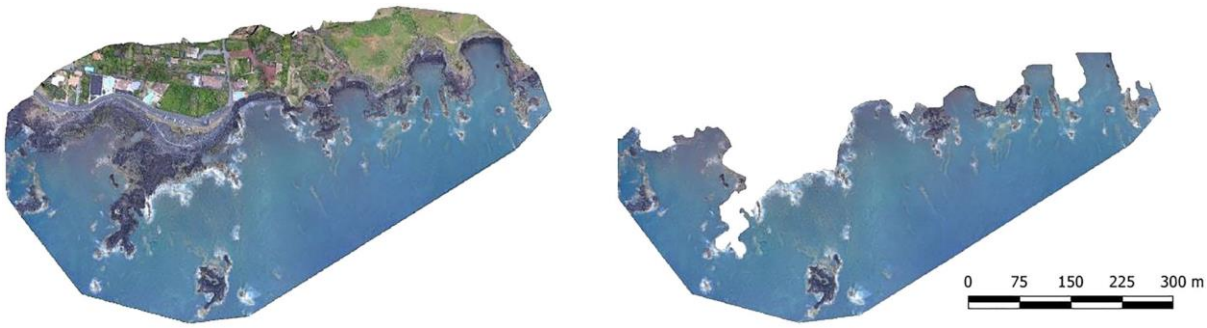

752

753 **FIGURE 3** Aerial and underwater (top right) view of *A. armata* samples in Mosteiros

754

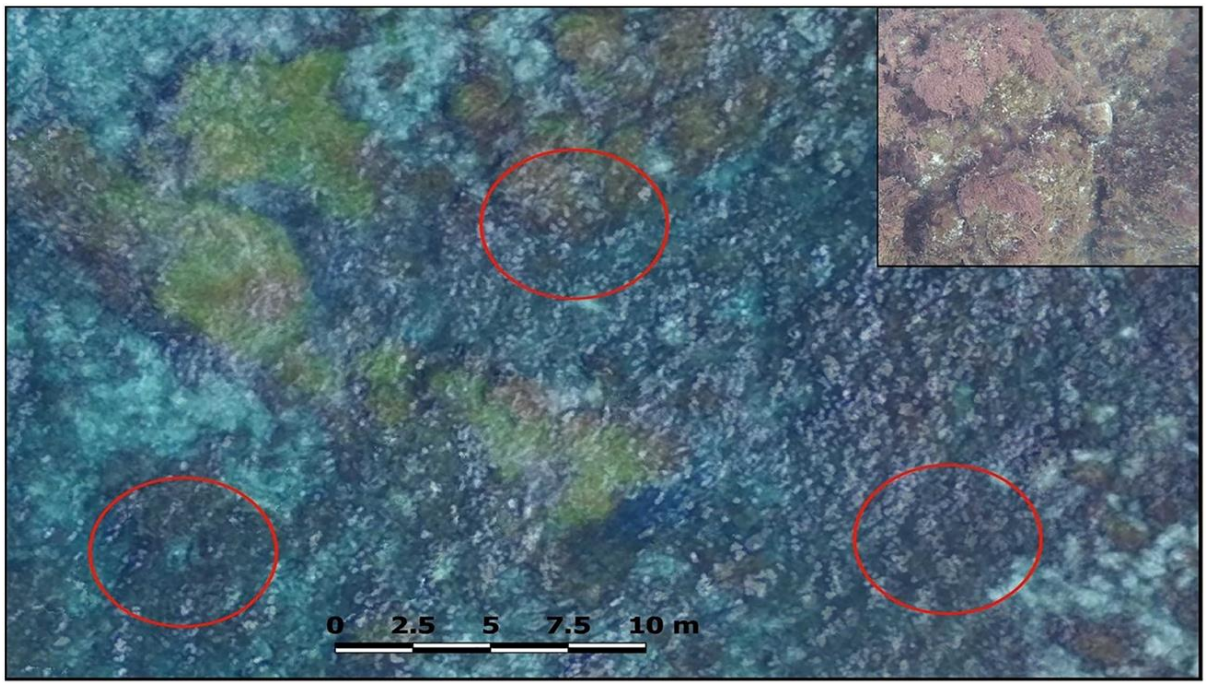

755

FIGURE 4 Mean (dot) and standard deviation (line) of RGB values per class

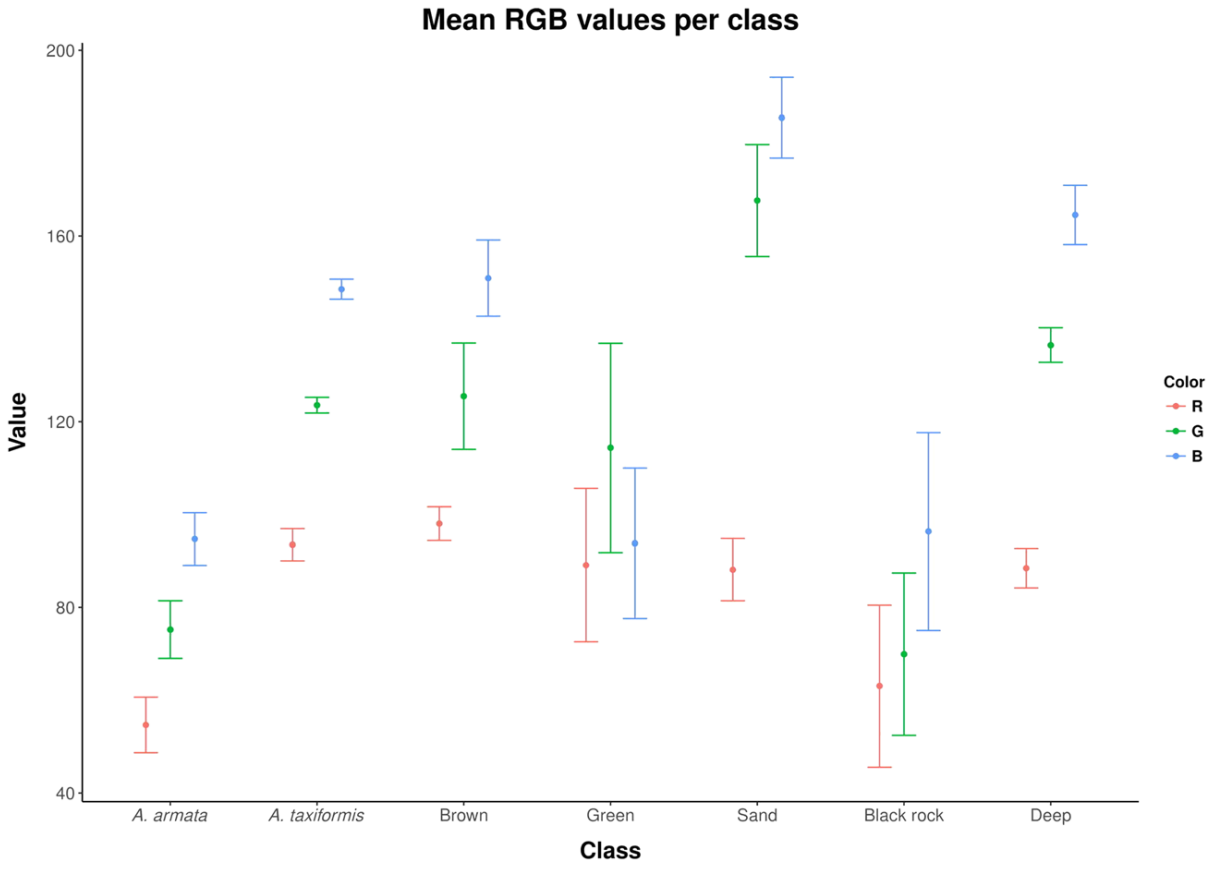

759 **FIGURE 5** Original masked image (above) and ANN model projection (below) for Lagoa

760

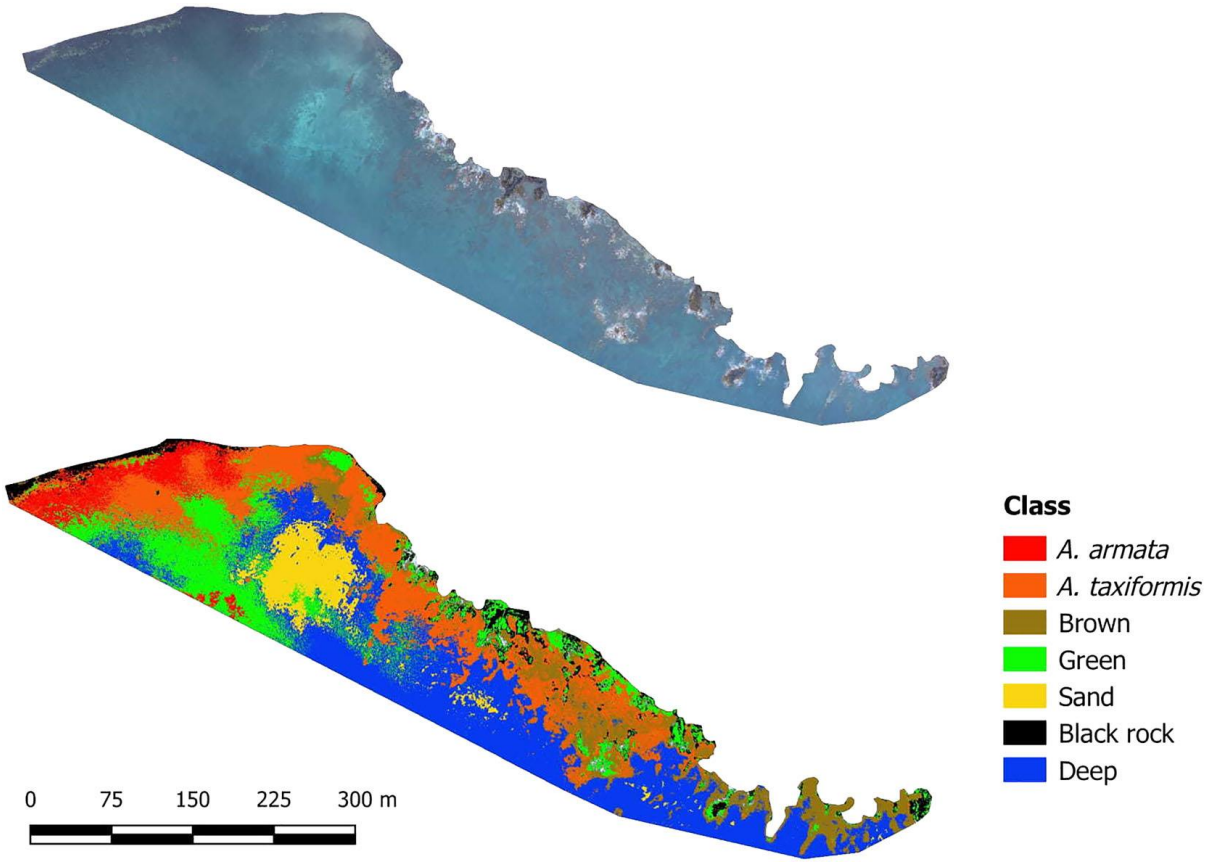

761

762 **FIGURE 6** Class proportions predicted by ANN, RF and SVM in Lagoa. The numbers within the bars
763 display area (m^2), estimated with the S.1 formula (supplementary information)
764

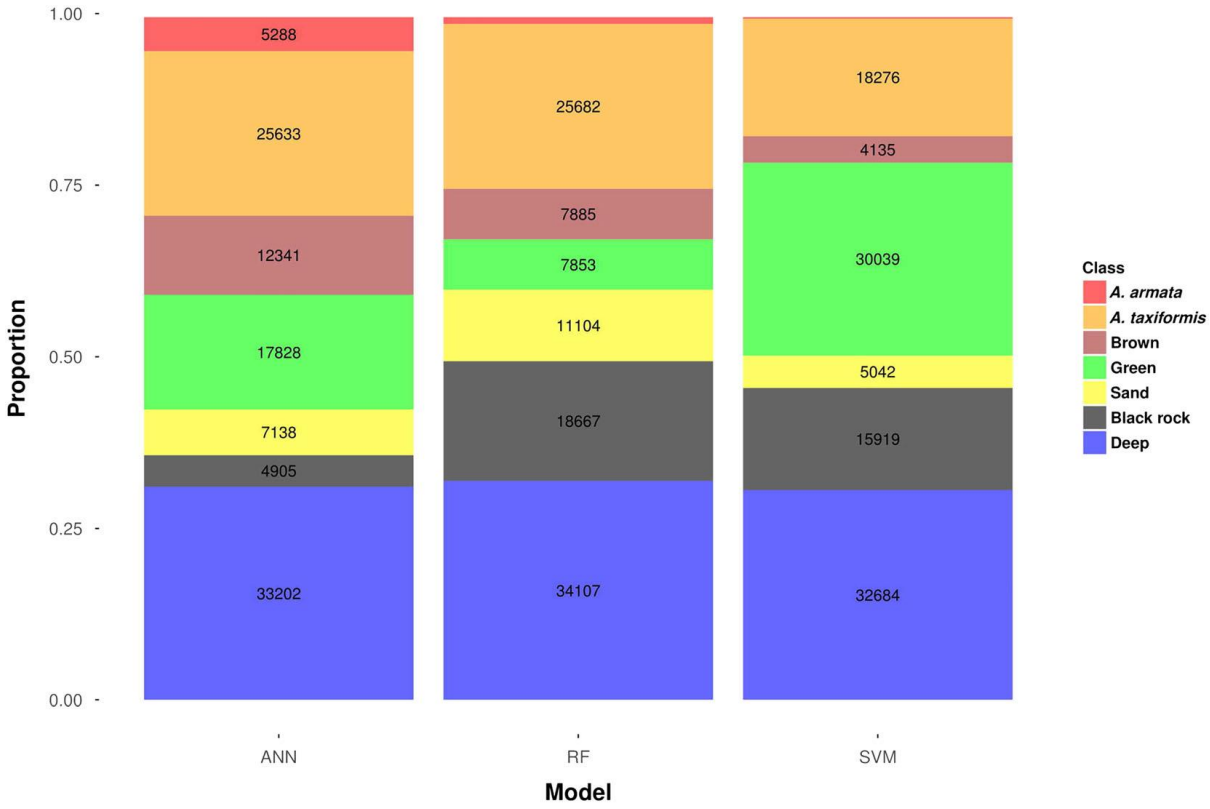

765
766
767